Catalysis Today 147 (2009) 239–246

Contents lists available at ScienceDirect

Catalysis Today

journal homepage: www.elsevier.com/locate/cattod

Hydrodeoxygenation of guaiacol on noble metal catalysts

A. Gutierrez *, R.K. Kaila, M.L. Honkela, R. Slioor, A.O.I. Krause

Helsinki University of Technology, Department of Biotechnology and Chemical Technology, P.O. Box 6100, FI-02015 Espoo, TKK, Finland

ARTICLE INFO

Article history:
Available online 16 December 2008

Keywords:
Pyrolysis oil
Upgrading
HDO
Noble metal catalysts

ABSTRACT

Hydrodeoxygenation (HDO) performed at high temperatures and pressures is one alternative for upgrading of pyrolysis oils from biomass. Studies on zirconia-supported mono- and bimetallic noble metal (Rh, Pd, Pt) catalysts showed these catalysts to be active and selective in the hydrogenation of guaiacol (GUA) at 100 °C and in the HDO of GUA at 300 °C. GUA was used as model compound for wood-based pyrolysis oil. At the temperatures tested, the performance of the noble metal catalysts, especially the Rh-containing catalysts was similar or better than that of the conventional sulfided $CoMo/Al_2O_3$ catalyst. The carbon deposition on the noble metal catalysts was lower than that on the sulfided $CoMo/Al_2O_3$ catalyst. The performance of the Rh-containing catalysts in the reactions of GUA at the tested conditions demonstrates their potential in the upgrading of wood-based pyrolysis oils.

1. Introduction

Biomass has been proposed as a feedstock for fuels and chemicals in response to the imminent depletion of fossil fuels and the increasing concern over environmental protection. The chemical energy stored in biomass can be accessed directly by combustion or indirectly by converting it to a gas or liquid fuel. The fuel gas obtained from biomass gasification can be combusted for heat generation, in an engine or turbine it can be used to generate electricity, and after purification it can be converted to liquid fuels [1,2]. Liquid fuels can replace mineral oil in heat and electricity generation or they can be used in the production of specialty and commodity chemicals. Many processes that transform biomass to liquid fuels start with the thermal breakdown of chemical substances producing the so-called bio-oils [3]. The final bio-oils have higher energy density than raw biomass, which makes them more suitable for industrial applications [4]. Furthermore, they are CO_2 neutral, and their use does not generate SO_x emissions because the sulfur content of biomass is usually negligible [3].

Pyrolysis oils obtained from the fast pyrolysis of wood are complex mixtures of reactive chemical compounds (carboxylic acids, aldehydes, ketones, carbohydrates, degraded lignin), water (up to 25%), and some alkaline metals (Na, K, Mg, Ca) [2,3,5–7]. Degraded lignin is a mixture of over 30 different phenols [3,8–10].

Pyrolysis oils, and bio-oils in general, have lower heating value than mineral oils; they are incompatible with conventional fuels, and they are characterized by high viscosity and solid content [2]. Furthermore, the high concentration of oxygenated compounds (close to 40% oxygen) [3] makes pyrolysis oils chemically unstable [2,4]. The aim in upgrading these oils is to convert the oxygenated groups [4,11] so as to increase the thermal and chemical stability, heating value, and volatility [12]. The total or partial removal of oxygenates from pyrolysis liquids can be performed by decarboxylation (CDO, Eq. (1)), thermal cracking (CRA, Eq. (2)), hydrodeoxygenation (HDO, Eq. (3)) or a combination of these processes [5]. The idealized stoichiometric equations are as follows [5]:

$$C_6H_8O_4 \rightarrow C_4H_8 + 2CO_2 \quad (CDO) \tag{1}$$

$$C_6H_8O_4 \rightarrow C_{4.5}H_6 + H_2O + 1.5CO_2 \quad (CRA) \tag{2}$$

$$C_6H_8O_4 + 7H_2 \rightarrow C_6H_{14} + 4H_2O \quad (HDO) \tag{3}$$

In HDO performed at high temperatures and pressures in the presence of a catalyst, the reaction products separate into a hydrocarbon and a water phase [2,4,12,13]. The water present in the pyrolysis oil together with the water generated during the HDO reaction may have an adverse effect on the lifetime of the catalyst [13,14]. Also, compounds produced in the thermal degradation of lignin, such as guaiacol (GUA, 2-methoxyphenol) and substituted guaiacols, tend to form heavy hydrocarbons and coke which reduce the activity of the catalyst [12,15,16]. H_2 consumption is also a disadvantage in the HDO of pyrolysis oils [5]. According to Bridgwater [14], 62 kg of H_2 is required to hydrodeoxygenate one tonne of wood-based pyrolysis oil.

Sulfided Al_2O_3-supported CoMo and NiMo catalysts are used in the oil refineries in hydrotreating processes where the removal of S, N, O, and metals from oil streams and the saturation of hydrocarbons take place. The Al_2O_3 support is known to be active

* Corresponding author. Tel.: +358 9 451 2522; fax: +358 9 451 2622.
E-mail address: andrea.gutierrez@tkk.fi (A. Gutierrez).

0920-5861/$ – see front matter © 2008 Elsevier B.V. All rights reserved.
doi:10.1016/j.cattod.2008.10.037

for coke formation [11,12,16] and unstable in the presence of large amounts of water [17,18]. Sulfur stripping from the surface of the catalyst occurs in HDO applications causing deactivation of the catalyst and contamination of the products [13,19,20]. Since these problems apply in greater degree to the HDO of pyrolysis oils, the large-scale use of these catalysts in refineries would be challenging. The performance of the conventional catalysts can be improved by changing the support to a less acidic one, e.g., active carbon or silica, as reported by Centeno et al. [12]. Another approach for the HDO of pyrolysis oils is to design new catalysts, which are active at low temperatures needed to prevent coke formation. One option is to use reduced metal catalysts that can be produced on supports such as zirconia (ZrO_2), titania (TiO_2) and active carbon which tolerate water better than Al_2O_3 does [5,13,17,21].

We studied the upgrading of wood-based pyrolysis oils by HDO. GUA was selected as the model compound as it, and substituted guaiacols, are present in high concentration (up to 3 wt%) in pyrolysis oils and their thermal stability is low [8,11,12,15,18]. The results for mono- and bimetallic (Rh, Pt, Pd) ZrO_2-supported catalysts are compared with those for conventional HDO catalyst (Al_2O_3-supported sulfided CoMo), the ZrO_2 support, and non-catalytic experiments.

2. Experimental

2.1. Catalyst preparation and pretreatment

Monometallic Rh, Pd, and Pt catalysts and bimetallic RhPd, RhPt, and PdPt catalysts were prepared by dry impregnation on the ZrO_2 support. The ZrO_2 (MEL Chemicals EC0100) was ground to 0.25–0.42 mm and calcined at 900 °C for 16 h (5 °C/min from 30 to 900 °C). The monometallic catalysts Rh, Pt, and Pd were prepared by impregnation of the metal precursors, and the bimetallic catalysts RhPt and RhPd by co-impregnation. The bimetallic PdPt catalyst was prepared by the separate impregnation of the metal precursors because their mixture formed a precipitate making the co-impregnation procedure inappropriate. The precursors were $Pt(NH_3)_2(NO_2)_2$ (Aldrich, 3.4 wt% in dilute ammonium hydroxide), $Rh(NO_3)_3$ (Aldrich, 10 wt% Rh in >5 wt% nitric acid), and $Pd(NO_3)_2$ (Aldrich, 99.95% metal basis, 12–16 wt% Pd). After the impregnation the catalysts were dried at room temperature for 4 h and then at 100 °C overnight. Subsequently, the catalysts were calcined at 700 °C for 1 h (1.3 °C/min from 30 to 700 °C). A commercial hydrotreating catalyst $CoMo/Al_2O_3$ was ground and sieved to particle size 0.25–0.42 mm and used in the sulfided form.

All catalysts were pretreated in situ in batch at 400 °C. The catalysts were first dried with 1 MPa of air (AGA, 99.999%) for 1 h. After drying, the noble metal catalysts were reduced with 1 MPa of H_2 (AGA, 99.999%) for 1 h and the $CoMo/Al_2O_3$ catalyst was sulfided with 1 MPa of 5 vol% H_2S in H_2 for 1 h (AGA, 99.999%).

2.2. Catalyst characterization

The metal loading of the fresh catalysts was determined with an X-ray fluorescence spectrometer (Philips PW 1480 XRF) equipped with UniQuant 4 software. The N_2 physisorption and H_2 chemisorption of the fresh catalysts were determined with a Coulter Omnisorp 100 CX. The setup is explained in detail elsewhere [22,23]. The amounts of irreversibly chemisorbed H_2 were used as an indication of the total active surface of the catalysts.

The temperature-programmed reduction (H_2-TPR) of the noble metal catalysts was carried out with Altamira Instruments AMI-200R characterization equipment. Catalyst samples (80 mg) were flushed with Ar (Aga, 99.999%), heated from 30 to 160 °C at a rate of 10 °C/min, and held at 160 °C for 30 min. Then, the samples were heated from 160 to 700 °C at a rate of 15 °C/min under a flow of 20% O_2 (AGA, 99.999%) in He (AGA, 99.996%) and kept at 700 °C for 60 min. The samples were cooled to 50 °C in 20% O_2 in He flow. TPR was performed at a heating rate of 10 °C/min up to 700 °C under a flow (30 cm^3/min (NTP)) of 5% H_2 in Ar (Aga, 99.999%). The consumption of H_2 was monitored by a thermal conductivity detector (TCD).

Scanning electron microscopy (SEM) images were used to determine the success of the impregnation procedure and the effect of the testing conditions on the surface of the catalyst. The measurements were performed with a LEO 1450 SEM. Back-scattered electron detectors were used to record images at several magnifications. For the purpose of measurement, the particles of the fresh and used catalysts were attached to a double-sided carbon tape and coated with 10–15 nm layer of carbon.

2.3. Catalyst testing

Testing of the catalysts (0.3 g) was performed in a 40-ml stainless steel batch reactor. A solution of 3 wt% GUA (Sigma, >99%) in solvent (n-hexadecane, Sigma, >99%) was used to simulate the pyrolysis oil. After the pretreatment of the catalyst, 10 ml of the GUA solution was charged to the reactor. The pressure in the reactor was increased with H_2, after which the reactor was placed in a sand bath preheated to the desired reaction temperature (100 or 300 °C) and the pressure increased to the reaction pressure (8 MPa).

All the catalysts were tested at 100 °C for 5 h and at 300 °C for 3 h. The effect of the reaction time (1–5 h) was studied only with Rh/ZrO_2. After the reaction, the reactor was cooled down to room temperature and gas and liquid samples were taken. Gas samples were analyzed by gas chromatography (GC) and liquid samples by gas chromatography/mass spectrometry (GC/MS).

The amount of carbon deposited on the catalysts and the sulfur content of the fresh and used $CoMo/Al_2O_3$ catalyst were determined with a Leco SC-444 Carbon Sulfur analyzer. The samples were washed in xylene and dried overnight at 100 °C. For the carbon and sulfur determinations, the samples were treated in O_2 at 1350 °C.

2.4. Analysis of products

The compounds in the liquid phase were identified with a GC/MS (HP 1 fused silica capillary column, 50 m × 0.32 mm, film thickness of 0.52 μm). The quantification was performed with a GC equipped with a flame ionization detector (FID) and an HP 1 fused silica capillary column (60 m × 0.25 mm, film thickness of 1 μm). n-Decane (Fluka, >98%) was used as a standard in the quantification of reactants and products.

The samples from the gas phase were analyzed after their dilution with N_2 using four different GCs. The measurement of H_2 was performed with a GC equipped with a TCD and a molecular sieve column. O_2, N_2, CH_4, CO, and CO_2 were measured with a GC equipped with TCD, FID, and two columns, a Porapak N column for the determination of CO_2 and a molecular sieve column for the determination of O_2, N_2, CH_4, and CO. A third GC, equipped with FID and an Al_2O_3 "M" PLOT column was used to measure C_2–C_7 hydrocarbons. The sulfur-containing compounds of the gas phase were determined with a GC equipped with flame photometric detector and GS-Q column (30 m, 0.32 mm, trap 2.5 m, and 0.32 mm internal diameter). The results of the gas phase analysis were used only for qualitative purposes.

2.5. Data analysis

The conversions of GUA and the product distributions were calculated from the analyzed liquid phase. The conversion of GUA (X_{GUA} (%)) was calculated from the initial and final amounts (mol) of GUA (Eq. (4)). The unreacted GUA was not included in the calculation of the product distribution (P (mol%)) (Eq. (5)). In Eqs. (4) and (5), n represents the moles of the reactant or product.

$$X_{GUA}(\%) = \frac{n(\mathrm{GUA})_{IN} - n(\mathrm{GUA})_{OUT}}{n(\mathrm{GUA})_{IN}} \times 100 \quad (4)$$

$$P_i(\%) = \frac{n(\mathrm{product})_i}{\sum_{i=j}^{m} n(\mathrm{product})_i} \times 100 \quad (5)$$

The O/C and H/C molar ratios for the GUA feed are 0.29 and 1.14 mol/mol, respectively. After the HDO reaction, the O/C molar ratio of the product mixture should be lower than the O/C molar ratio of the reactant due to the elimination of oxygen. Furthermore, the H/C molar ratio should increase because hydrogenation reactions are taking place. Thus, the O/C and H/C molar ratios (Eqs. (6) and (7), n represents number of moles) of the product mixture can be used to assess the success of the HDO, where values close to those of gasoline and diesel (O/C = 0–0.002 and H/C = 1.8–2.0 mol/mol [24]) are desired. The unreacted GUA in the reaction mixture after 3 or 5 h reaction was included in the calculation of the O/C and H/C molar ratios.

$$O/C(\mathrm{mol/mol}) = \frac{\sum n(\mathrm{oxygen})_{\text{unreacted GUA and products}}}{\sum n(\mathrm{carbon})_{\text{unreacted GUA and products}}} \quad (6)$$

$$H/C(\mathrm{mol/mol}) = \frac{\sum n(\mathrm{hydrogen})_{\text{unreacted GUA and products}}}{\sum n(\mathrm{carbon})_{\text{unreacted GUA and products}}} \quad (7)$$

3. Results and discussion

3.1. Catalyst properties

The metal loadings of the mono- and bimetallic catalysts determined by XRF are presented in Table 1. The low temperatures (100 and 300 °C) used here in the testing of the catalysts are not expected to cause metal leaching.

The properties determined for the mono- and bimetallic catalysts (BET surface areas (m^2/g), total pore volumes (cm^3/g), and irreversible H_2 chemisorption) are presented in Table 2. BET surface areas and total pore volumes above 0.1 nm were similar for the catalysts and the support calcined at 900 °C. Thus, the calcination of the catalysts performed at 700 °C had no effect on the catalyst structure.

On the surface of the fresh bimetallic PdPt catalyst small clusters were detected (Fig. 1A). For the other noble metal catalyst the SEM images revealed no metal clusters on the surface after the calcinations; only the ZrO_2 support was visible. This suggests a successful impregnation procedure or the encapsulation of the metal within the support material [25,26].

Table 1
Metal loadings of the fresh ZrO_2-supported noble metal catalysts.

	Metal loading		
	Rh	Pd	Pt
Pt	–	–	0.73
Pd	–	0.25	–
Rh	0.39	–	–
RhPt	0.25		0.25
RhPd	0.25	0.12	
PdPt	–	0.14	0.32

Table 2
Physisorption and chemisorption results for the fresh noble metal catalysts.

Catalyst	BET (m^2/g_{cat})	Total pore volume above 100 nm (cm^3/g_{cat})	Irreversible chemisorption of H_2 ($\mu mol/g_{cat}$)
ZrO_2	20[a]	0.19[b]	1.5[a]
Pt	17[a]	0.15[b]	0.13[a]
Pd	17	0.080	1.2
Rh	20[a]	0.096[b]	3.1[a]
RhPt	23[b]	0.092[b]	4.3[b]
RhPd	21	0.091	1.2
PdPt	16	0.085	0.96

[a] Ref. [23].
[b] Ref. [22].

Irreversibly chemisorbed H_2 ($\mu mol/g_{cat}$) for the different catalysts is reported in Table 2. The metal dispersion cannot be calculated based on these data for the noble metal catalysts tested as the H_2 adsorption can be dissociative or non-dissociative. Moreover, for the bimetallic catalysts the metal molar ratio and the fact that the interaction between the metals might affect the H_2 adsorption should be taken into consideration. Because the irreversibly chemisorbed H_2 is an indication of the active surface of a material, based on the results reported in Table 2 some catalytic activity is expected for the support. Thus, the support also contributes to the total H_2 chemisorption. The lowest irreversible H_2 uptake was measured for the monometallic Pt catalyst (Table 2) [23]. The H_2 uptake was markedly improved in the bimetallic RhPt catalyst when compared to the results obtained for monometallic catalysts, indicating the interaction of these two metals. The combination of Rh and Pd in the RhPd catalyst and the combination of Pd and Pt in the PdPt catalyst, in turn, did not improve the irreversible H_2 uptake over that of the monometallic catalysts, and the values measured were similar to that of the support.

The H_2-TPR results are presented in Fig. 2, where the H_2 consumption is shown as a function of temperature. The H_2-TPR of the monometallic Rh catalyst showed one main reduction step at 117 °C, and a minor step at 210 °C. No reduction steps were detected on the Pt catalyst. That is, no reducible species of Pt are formed at the high calcination temperature (700 °C) that was used [22,27,28]. One reduction step at 300 °C was detected for the monometallic Pd catalyst. All the catalysts presented a reduction step at 560–580 °C, which corresponded to the reaction of H_2 with oxygen atoms present in the ZrO_2 support [29].

Two reduction steps were detected for the bimetallic RhPd catalyst (Fig. 2) and both steps corresponded to those detected for the monometallic Rh catalyst while the reduction peak of Pd was not present. For the RhPt catalyst, only one of the reductions steps of Rh was identified but the width of the step suggests the overlapping with second reduction step (210 °C). Only one reduction step was present for the PdPt catalyst and it corresponded to the reduction step of Pd. The differences in the shapes of the peaks obtained for the monometallic and for the bimetallic catalysts suggest that there is interaction between the metals in the bimetallic catalysts.

3.2. Solubility of hydrogen and water in the reaction mixture

The solubility of H_2 in the liquid phase is essential for the reactions of GUA to take place. The solubility of H_2 in the solvent (n-hexadecane) was estimated for the experimental conditions using Flowbat software [30] and the Boston–Mathias modification of the α-term (no binary interaction parameters) of the Soave

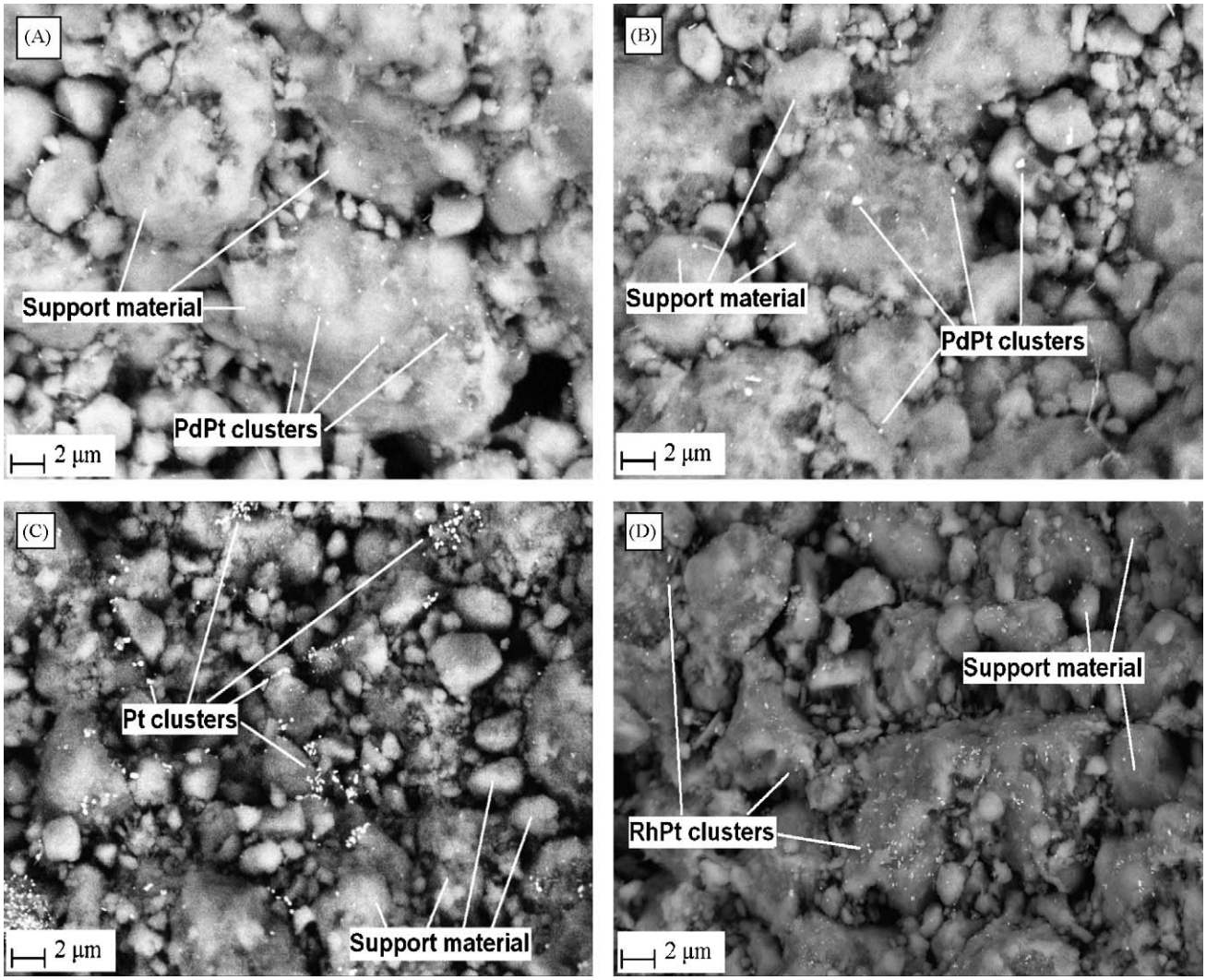

Fig. 1. SEM images of fresh and tested catalysts (HDO of GUA at 100 °C, 8 MPa, 5 h). (A) Fresh PdPt, (B) tested PdPt, (C) tested Pt and (D) tested RhPt.

modification of the Redlich–Kwong (SRK) equation of state. In view of the low concentration of GUA (3 wt%), the solubility of H_2 in n-hexadecane was assumed to represent the solubility of H_2 in the reaction mixture. The critical properties used in the simulations were T_c = –239.95 °C, P_c = 1.3 MPa, and ω = –0.2180 for H_2 and T_c = 449.85 °C, P_c = 1.4 MPa, and ω = 0.7471 for n-hexadecane [30].

Under the experimental conditions, 100 and 300 °C at 8 MPa, the estimated solubilities were 0.42 and 0.97 mol H_2/kg of n-hexadecane, respectively. These values are in agreement with the reported experimental values, 0.40 mol H_2/kg at 100 °C and 0.90 mol H_2/kg at 300 °C [31]. From the amount of GUA (0.002 mol) in the reactor, and assuming complete deoxygenation and hydrogenation of GUA into cyclohexane, methane, and water (Eq. (8)), the required amount of H_2 (H_2 HDO) was calculated to be 0.01 mol.

$$C_7H_8O_2 + 6H_2 \rightarrow C_6H_{12} + CH_4 + 2H_2O \quad (8)$$

Table 3 presents the experimental conditions for the reactions of GUA. Excess H_2 was fed to the reactor as indicated by the ratio H_2 fed/H_2 HDO. In the equilibrium only a small fraction of H_2 is in the liquid phase (H_2 in liquid, Table 3). However, H_2 limitation was not expected to take place in the liquid phase owing to the vigorous agitation and sufficiently long reaction times that ensure that the equilibrium for H_2 is reached.

Water is produced through the removal of oxygen from the GUA molecule (Eq. (8)) and thus separate phases for hydrocarbons and water are expected after the reaction. In our experiments only small amounts of water (0.067 g of water assuming complete HDO of the GUA) are expected because of the small amount of GUA (0.23 g GUA in 7.5 g hexadecane) in the reactor. The liquid–liquid equilibrium in the reaction mixture was estimated for the sampling conditions (room temperature and pressure) using the Dortmund-modified UNIFAC in the Flowbat software [30]. According to the estimation, the total amount of water that can be dissolved in the mixture of GUA and hexadecane is 0.0063 g [30]. The water solubility may be higher, however, because of the products present in the mixture after the reaction.

3.3. HDO of GUA at 300 °C

The conventional hydrotreating catalyst (sulfided $CoMo/Al_2O_3$) and the ZrO_2-supported noble metal catalysts were tested in the HDO of GUA at 300 °C and 8 MPa for 3 h. These experimental conditions are the ones typically used with the conventional sulfided Al_2O_3-supported CoMo catalyst [10,12,15,16,32]. Non-

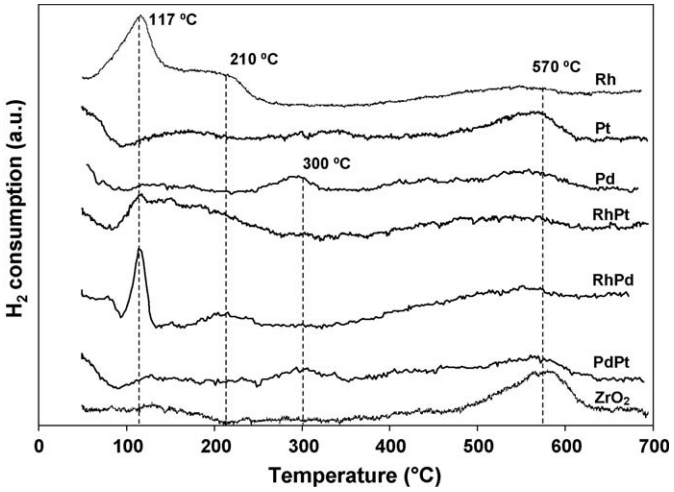

Fig. 2. H_2-TPR profiles for the mono- and bimetallic noble metal catalysts calcined at 700 °C for 1 h.

Table 3
Experimental conditions for HDO of GUA.

GUA (mol)[a]		0.002
Solvent (n-hexadecane)[a] (mol)		0.033
H_2 HDO[b] (mol)		0.01
	T (°C)	
	100	300
H_2 initial (mol)[a]	0.11	0.07
H_2 in liquid (mol)[c]	0.003	0.007
H_2 initial/H_2 HDO (mol/mol)	9.55	6.37
H_2 in liquid/GUA (mol/mol)	1.73	4.02
H_2 in liquid/H_2 HDO (mol/mol)	0.29	0.67

[a] Initial amount in the reactor.
[b] Amount of H_2 required to complete HDO of the GUA molecule yielding cyclohexane, water, and CH_4 as products.
[c] Estimated considering the H_2 solubility in n-hexadecane under the experimental conditions.

catalytic experiments and experiments with ZrO_2 were performed for comparison.

3.3.1. Conventional sulfided $CoMo/Al_2O_3$

The conversion of GUA was complete and the production of benzene predominated in the reaction at 300 °C on the conventional sulfided $CoMo/Al_2O_3$ catalyst. Sulfur leached from the catalyst during the reaction, as seen in the decrease of the carbon-free sulfur content from 8.2 wt% for the fresh catalyst to 5.1 wt%. Leached sulfur was responsible for the contamination of the products, as methanethiol and dimethyl sulfide were detected in the gas phase and cyclohexanethiol and methylthiocyclohexane in the liquid phase.

Şenol et al. [19] reported a decrease in the sulfur content of the $CoMo/Al_2O_3$ catalyst in the HDO of aliphatic esters performed in a continuous reactor at 250 °C and 1.5 MPa. They also found that the sulfur content of the $CoMo/Al_2O_3$ catalyst remained constant in the HDO of phenol under the same experimental conditions [20]. This difference between aliphatic and aromatic compounds in the absence of sulfiding agent, and also between phenol and GUA, suggests that sulfur-containing compounds play different roles in HDO.

The carbon deposition on the used $CoMo/Al_2O_3$ catalyst was 10 wt%. Carbon deposition would be expected to be higher in the HDO of real pyrolysis oil making the application of sulfided catalysts at industrial scale highly challenging.

3.3.2. ZrO_2-supported noble metal catalysts

In the experiments at 300 °C, all the noble metal catalysts gave complete or almost complete conversion of GUA and the deoxygenation of GUA was catalyzed. The main product was benzene, and also small amounts of cyclohexanol were produced. In noncatalytic experiments and with the ZrO_2 support, the conversions of GUA were 13% and 27%, respectively, and the main product was cyclohexanol.

O/*C* and *H*/*C* molar ratios were used to characterize the product mixture. These are presented in Fig. 3. In noncatalytic experiments and with the ZrO_2 support, the ratios scarcely changed during the 3 h experiments. The *O*/*C* molar ratio decreased with all the catalysts, and values close to those of gasoline and diesel were reached with the Rh, RhPd, and sulfided $CoMo/Al_2O_3$ catalysts demonstrating their high selectivity for deoxygenation reactions. The *H*/*C* molar ratio of gasoline and diesel was not reached and the values achieved were close to that of the main product, benzene.

The high activity of the noble metal catalysts at 300 °C made it difficult to compare them. Instead, the comparison was performed at 100 °C where the conversion of GUA was incomplete.

3.4. Reactions of GUA at 100 °C

ZrO_2-supported mono- and bimetallic noble metal (Rh, Pd, and Pt) catalysts were tested at 100 °C and 8 MPa for 5 h. The results with these catalysts were compared with those for the ZrO_2 support, the sulfided $CoMo/Al_2O_3$ catalyst, and with the noncatalytic experiment. In further experiments, the reactions of GUA on the monometallic Rh catalyst were studied as a function of time.

3.4.1. Catalytic activity

The conversions of GUA obtained in noncatalytic and catalytic experiments at 100 °C are presented in Table 4. The presence of catalyst improved the conversion over that obtained with ZrO_2 and in the noncatalytic experiment. GUA conversions with the monometallic Pd and Pt catalysts were similar to the conversion achieved with the sulfided $CoMo/Al_2O_3$ catalyst (13.8%), and complete conversion of GUA was obtained with the monometallic Rh catalyst. The low active surface area suggested by the low H_2

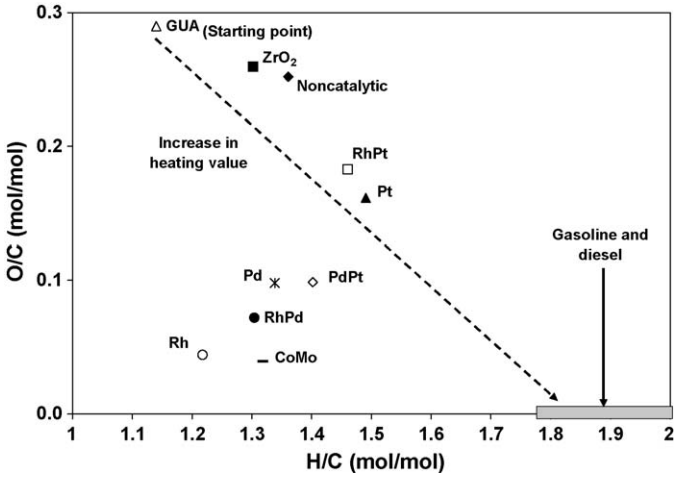

Fig. 3. *O*/*C* and *H*/*C* molar ratios of GUA products obtained in a thermal experiment and with ZrO_2, ZrO_2-supported noble metal catalysts, and a conventional HDO catalyst at 300 °C, 8 MPa and 3 h.

irreversible chemisorption (Table 2) could explain the low activity of the Pt and Pd catalysts. In addition, the large active surface area and good metal dispersion indicated by the H_2 irreversible chemisorption and SEM images of the fresh catalyst could explain the high activity of the Rh catalyst.

In relation to the monometallic catalysts, the combination of Pd and Pt in the bimetallic PdPt catalyst had an adverse effect on the conversion of GUA as the conversion reached with the PdPt catalyst was similar to the one obtained in the noncatalytic experiment and with the support (Table 4). This is in agreement with the low irreversible H_2 chemisorption measured for the PdPt catalysts that predicted a low active surface area (Table 2). The combination of Pd or Pt with Rh, on the other hand, improved the GUA conversion from values around 10% for the monometallic catalysts to 32.7% on the RhPd and 98.7% on the RhPt catalyst (Table 4). The conversions obtained with the bimetallic catalysts could not be predicted from the conversions achieved with the monometallic catalysts. This supports the conclusion that Pd and Pt interact with Rh which was also predicted by the TPR measurements (Fig. 2).

The SEM images for the PdPt, Pt, and RhPt catalysts tested at 100 °C are presented in Fig. 1B, C, and D, respectively. Some metal sintering was detected for these catalysts, but no metal clusters were detected for the tested monometallic Rh catalyst. In our early work on similar noble metal catalysts [22] we found large metal clusters after the autothermal reforming. In the case of the RhPt catalyst, the clusters were identified as orthorhombic. After the present tests at 100 °C, the clusters were too small for the shape to be identified. However, the sintering reported after the testing of the Pt and PdPt catalysts could be responsible for the low activity (Fig. 1). However, the complete conversion achieved with the RhPt catalyst suggests that longer experiments are required to determine the effect of sintering on the performance of this catalyst.

The results reported in Table 4 show Rh to be the most active noble metal. The activity of the ZrO_2-supported Rh catalyst was therefore studied further at 100 °C with shorter reaction times (1–5 h). As presented in Fig. 4, the conversion of GUA increased from 45% to complete between 1 and 5 h. This indicates that the reactions of GUA at 100 °C are slower than at higher temperatures.

3.4.2. Reaction products

In all the experiments, the gas phase was composed mainly of unreacted H_2 and only minor amounts of benzene, toluene, and light hydrocarbons. Hence, the comparison of the catalysts was focused on the liquid phase.

Only one liquid phase was observed in our experiments, and no phase separation was detected in any of the samples over time. Small amounts of water were formed in the experiments at 100 °C; for example, for Rh, the most active catalyst, the amount of water (based on the oxygen elemental balance) was 0.015 g after 5 h. This amount is greater than the value calculated for the liquid–liquid equilibrium in the reaction mixture, but the solubility of water may be higher in the presence of the products. Under the sampling conditions (room temperature and pressure), a part of the water formed during the reaction may be in the gas phase (vapor equilibrium).

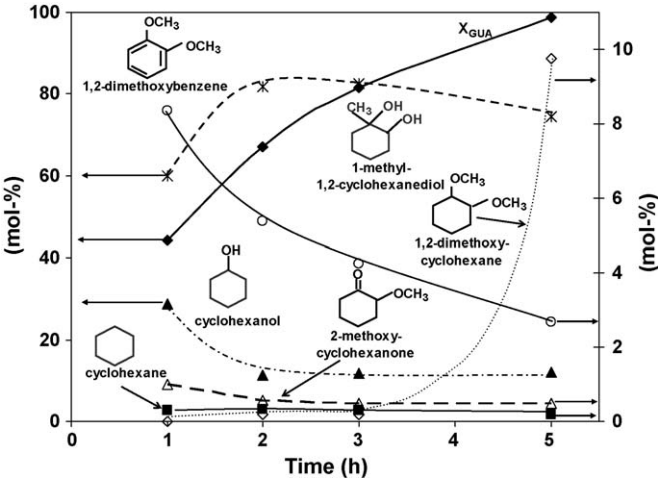

Fig. 4. GUA conversion and distribution of main products for experiments with Rh/ZrO_2 at 100 °C, 8 MPa and 1–5 h.

Fig. 5 presents the distribution of the main products for the catalytic and noncatalytic experiments at 100 °C after 5 h. Because of the large number of products in the liquid phase, only the amounts of the main products (1-methyl-1,2-cyclohexanediol, cyclohexanol, 1,2-dimethoxybenzene, and cyclohexane) are compared. Methylcyclopentane, methylcyclohexane, methoxycyclohexane, cyclohexanone, cyclopentanemethanol, 2-methoxycyclohexanone, 1,2-dimethoxycyclohexane, and 1,1-dicyclohexane are reported as other hydrogenated products (*other hydr.*). Also, toluene, 1,2-dimethylbenzene, methoxybenzene, phenol, 2-methylphenol, 1,2-dihydroxybenzene (CAT) and benzene were detected, and the amounts were summed and are reported as other aromatic products (*other arom.*).

The products at 100 °C were mainly hydrogenated oxygen-containing compounds and we can conclude that there was no lack of H_2 in the liquid phase. Similar product distributions were obtained with the PdPt catalyst (Fig. 5), in the noncatalytic experiment, and with the ZrO_2 support, in accordance with the low GUA conversions (Table 4). Thus, thermal, noncatalytic reactions predominated in the presence of the PdPt catalyst.

Despite the similar GUA conversions obtained with the Pt, Pd, and sulfided $CoMo/Al_2O_3$ catalysts, the product distributions were clearly different (Fig. 5). The formation of cyclohexanol was higher on Pt and CoMo than on Pd, whereas the amount of 1-methyl-1,2-cyclohexanediol was highest on Pd and negligible on the sulfided $CoMo/Al_2O_3$. These results suggest that these catalysts are active for different reaction paths.

With the Rh-containing catalysts, the main product was 1-methyl-1,2-cyclohexanediol (Fig. 5). The amount of cyclohexanol was larger with the RhPd catalyst than with RhPt and Rh. GUA conversions and product distributions were similar with Rh and RhPt. Hence, part of the Rh in the Rh catalyst could be replaced with Pt without changing its catalytic performance.

The production of other aromatic compounds ("*other arom.*" in Fig. 5) and other hydrogenated compounds ("*other hydr.*" in Fig. 5) was similar for all except for the Rh-containing catalysts. There the

Table 4
Conversion of GUA and carbon deposition for noncatalytic and catalytic experiments at 100 °C, 8 MPa and 5 h.

	Noncatalytic	ZrO_2[a]	PdPt[a]	Pt[a]	Pd[a]	CoMo[b]	RhPd[a]	RhPt[a]	Rh[a]
X_{GUA} (%)	5.6	5.1	5.2	10.0	13.7	13.8	32.7	98.7	98.9
Carbon deposition (wt%)	–	0.5	0.4	0.6	0.7	6.7	1.0	1.0	1.8

[a] Pretreated (dried and reduced) at 400 °C.
[b] Pretreated (dried and sulfided) at 400 °C. Carbon-free sulfur content: fresh 8.2 wt% and used 7.4 wt%.

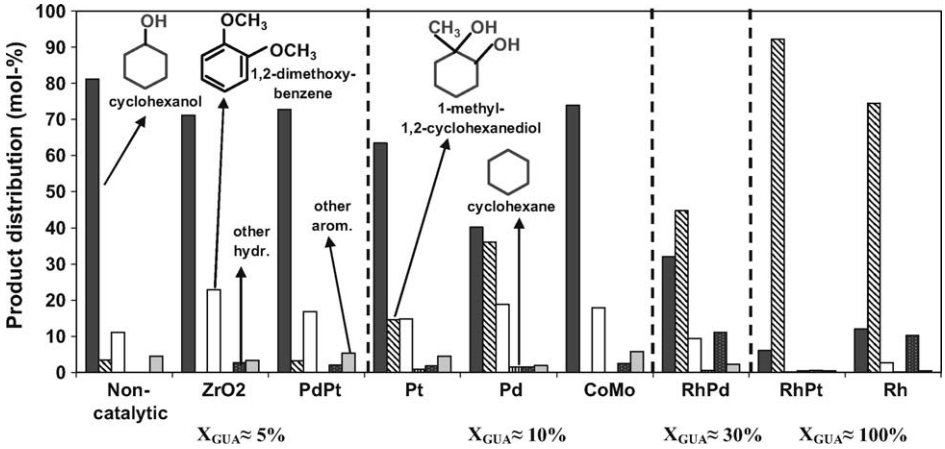

Fig. 5. Main product distribution for noncatalytic and catalytic experiments at 100 °C, 8 MPa and 5 h.

amounts of other aromatic compounds were negligible and the amount of other hydrogenated compounds were high (10 mol%). Negligible amounts of cyclohexane and benzene were produced on all catalysts indicating the high selectivity for hydrogenated oxygen-containing compounds (1-methyl-1,2-cyclohexanediol and cyclohexanol). As cyclohexanediols were also the main products in the reactions of substituted guaiacols at 150 °C and 13.5 MPa on Ru/C [17], there is some similarity in the catalytic performance of Ru/C with that of the presently tested noble metal catalysts.

The effect of the catalysts on the *O*/*C* and *H*/*C* molar ratios of the product mixture (products and unreacted GUA) was examined. After 5 h at 100 °C, similar *O*/*C* ratios to that of the GUA (0.29 mol/mol) were obtained with all catalysts. Thus, the catalytic effect on the deoxygenation of GUA was negligible, and oxygen removal was mainly due to thermal reactions. However, the Rh and RhPt catalysts had a considerable effect on the *H*/*C* molar ratio (1.95 mol/mol), and the values of gasoline and diesel were reached.

As presented in Fig. 4, in experiments performed with monometallic Rh catalyst and shorter reaction times (1–5 h) the main products were oxygen-containing compounds: 1-methyl-1,2-cyclohexanediol, cyclohexanol, and 1,2-dimethoxycyclohexane. Also, 1,2-dimethoxybenzene, 2-methoxycyclohexanone, and cyclohexane were produced. The concentration of the products stabilized after 2 h, except for 1,2-dimethoxybenzene and 1,2-dimethoxycyclohexane. The formation of 1,2-dimethoxybenzene decreased with time, while the production of 1,2-dimethoxycyclohexane was negligible from 1 to 3 h but increased drastically after 3 h suggesting that the noble metal catalysts are catalyzing consecutive reactions.

3.5. Effect of temperature on the reactions of GUA

The results presented above demonstrate a clear dependence of the product distribution on temperature. At 100 °C, the production of hydrogenated oxygen-containing compounds indicated that the reactions were not limited by H_2 availability in the liquid phase. At 300 °C, even though more H_2 should be available in the liquid phase, the main products were aromatic compounds. Hydrogenation of the aromatic ring predominated at 100 °C, while deoxygenation predominated at 300 °C. According to the ΔG° values calculated for the hydrogenation and deoxygenation reactions of GUA as a function of temperature, neither reaction is limited by thermodynamics [33]. However, saturation of the aromatic ring is favored at low temperatures [33].

The availability of H_2 on the catalyst surface at the different temperatures could affect the formation of products. H_2 adsorption is an exothermic reaction as indicated by the H_2-adsorption enthalpies calculated and measured by Jiang et al. [34] for mono- and bimetallic Al_2O_3-supported Pd- and Pt-containing catalysts. Thus, the H_2 equilibrium coverage decreases with increase in temperature, as also measured by Derrouiche and Bianchi [35] for a Pt/Al_3O_2 catalyst. In addition, the H_2 adsorption is affected by the atomic ratio of the metals in bimetallic catalysts [34]. Even with no detailed kinetics available, we can expect the hydrogenation and the deoxygenation of GUA to proceed with a positive reaction order for H_2. Thus, low H_2 coverage on the catalysts at high temperatures would reduce the reaction rates of both hydrogenation and deoxygenation. Still, more H_2 would be consumed in hydrogenation than in deoxygenation. This is in agreement with our results in which more deoxygenation than hydrogenation occurred at high temperatures.

Large amounts of 1-methyl-1,2-cyclohexanediol were formed at 100 °C with the noble metal catalysts but not with the sulfided $CoMo/Al_2O_3$ catalyst (Fig. 5). This means that, the methyl transfer to the hydrocarbon ring is catalyzed only at low temperatures by the noble metal catalysts.

3.6. Characterization of tested catalysts

The carbon deposition on the catalysts was measured after the tests at 100 °C (5 h). The results are presented in Table 4. Carbon deposition on the noble metal catalysts was lower than with the conventional sulfided $CoMo/Al_2O_3$ catalyst (6.7 wt%). The value was highest for the Rh catalyst (2 wt%) and lowest for the less active catalysts (PdPt, Pd, Pt). The carbon deposition on the less active catalysts was similar to that on the ZrO_2 support. Hence, the carbon deposition was directly related to the activity of the noble metal catalysts.

Increasing the reaction temperature increased the carbon deposition. In the tests at 300 °C, values were close to 2.6 wt% with the noble metal catalysts while the value was 10 wt% with the conventional sulfided $CoMo/Al_2O_3$ catalyst. The increase in carbon deposition with temperature is in agreement with the increase in cracking reactions caused by low H_2 coverage of the catalysts at high temperatures.

The sulfur content of the sulfided $CoMo/Al_2O_3$ catalyst (8.2 wt%) decreased to 5.1 wt% during testing at 300 °C but only to 7.4 wt% during testing at 100 °C. At 100 °C, the sulfur contaminated only the gas phase; no sulfided compounds were detected in the liquid phase.

4. Conclusions

ZrO_2-supported noble metal catalysts were studied in the reactions of GUA in the presence of H_2 at 100 and 300 °C. The results were compared with those for a conventional hydrotreating catalyst. With the conventional sulfided $CoMo/Al_2O_3$ catalyst, the products were contaminated with sulfur, and the catalyst deactivated due to carbon deposition. These are common problems with conventional sulfided hydrotreating catalysts. Neither problem was encountered with the ZrO_2-supported noble metal catalysts.

At 100 °C, hydrogenated oxygen-containing compounds were produced with all the catalysts tested. However, different reaction products were detected with the sulfided $CoMo/Al_2O_3$ and the noble metal catalysts. According to the product distributions, methyl transfer to the hydrocarbon ring was catalyzed with the noble metal catalysts but not with the conventional catalyst. The main difference between the mono- and bimetallic noble metal catalysts was in their activity.

Complete conversion of GUA was achieved on ZrO_2-supported Rh and RhPt catalysts at 100 °C. Furthermore, the *H*/*C* molar ratios achieved on these catalysts were similar to the *H*/*C* ratio for gasoline and diesel. Deoxygenation of GUA took place only at 300 °C, however, and desired low *O*/*C* ratios of gasoline and diesel were achieved with the Rh and RhPd catalysts.

Characterization results of the mono- and bimetallic noble metal catalysts suggest interactions between the metals. The interaction of Rh with Pt and Pd was evident in the H_2-TPR, chemisorption results and in the performance of the bimetallic catalysts (RhPt and RhPd). These bimetallic catalysts gave noticeably better results than the monometallic Pt and Pd catalysts and the results were not the average combination of the results obtained with the monometallic catalysts. In contrast to this, the combination of Pd and Pt in the bimetallic PdPt catalyst had an adverse catalytic effect on the reactions of GUA: the performance of the bimetallic catalyst was worse than that of the monometallic catalysts.

Rh-containing catalysts give good HDO and hydrogenation performance at high and low temperatures, respectively. The high activity of these catalysts in the reactions of GUA in the presence of H_2 indicates the potential for their use in the upgrading of wood-based pyrolysis oils.

Acknowledgments

This work was financed by EU project BIOCOUP (518312). The Technical Research Centre of Finland (VTT) is thanked for the help in setting up the reactor and the gas products analyses. Dr. Erkki Heikinheimo and Lassi Hiltunen are thanked for the SEM images and XRF determinations, respectively. Kati Vilonen, Arto Mäkinen, and Sonja Kouva are thanked for their help with the physisorption, chemisorption and TPR determinations. Dr. Kari Keskinen and Agnes Ardiyanti (University of Groningen, The Netherlands) are acknowledged for valuable discussions.

References

[1] A. Demirbaş, Energy Convers. Manage. 42 (2001) 1357.
[2] A.V. Bridgwater, S. Czrnik, J. Piskorz, in: A.V. Bridgwater (Ed.), Fast Pyrolysis of Biomass: A Handbook, Antony Rowe Ltd., Chippenham, UK, 2002, pp. 1–22.
[3] D. Mohan, C.U. Pittman, P. Steele, Energy Fuels 20 (2006) 848.
[4] P. Grande, E. Laurent, R. Maggi, A. Centeno, B. Delmon, Catal. Today 29 (1996) 297.
[5] S.R.A. Kersten, W.P.M. van Swaaij, L. Lefferts, K. Seshan, in: G. Centi, R.A. van Santen (Eds.), Catalysis for Renewables—From Feedstocks to Energy Production, Wiley–VCH, Weinheim, 2007, p. 119 (Chapter 6).
[6] A. Oasmaa, E. Kuoppala, Y. Solantausta, Energy Fuels 17 (2003) 433.
[7] J.H. Marsman, J. Wildschut, F. Mahfud, H.J. Heeres, J. Chromatogr. A 1150 (2007) 21.
[8] S.J. Hurff, M.T. Klein, Ind. Eng. Chem. 22 (1983) 426.
[9] H. Kawamoto, S. Horigoshi, S. Saka, J. Wood Sci. 53 (2007) 168.
[10] E. Laurent, B. Delmon, Ind. Eng. Chem. Res. 32 (1993) 2516.
[11] E. Furimsky, Appl. Catal. A 199 (2000) 147.
[12] A. Centeno, E. Laurent, B. Delmon, J. Catal. 154 (1995) 288.
[13] A. Bridgwater, Appl. Catal. A 116 (1994) 5.
[14] A.V. Bridgwater, Catal. Today 29 (1996) 285.
[15] E. Laurent, B. Delmon, Appl. Catal. A 109 (1994) 97.
[16] G. de la Puente, A. Gil, J.J. Pis, P. Grange, Langmuir 15 (1999) 5800.
[17] D.C. Elliot, G.G. Neuenschwander, T.R. Hart, J. Hu, A.E. Solana, C. Cao, in: A.V. Bridgwater, D.G.B. Boocock (Eds.), Science in Thermal and Chemical Biomass Conversion, vol. 2, CPL Scientific Ltd., Newbury, 2006, p. 1536.
[18] E. Furimsky, F.E. Massoth, Catal. Today 52 (1999) 381.
[19] O.İ. Şenol, T.-R. Viljava, A.O.I. Krause, Appl. Catal. A 326 (2007) 236.
[20] O.İ. Şenol, E.-M. Ryymin, T.-R. Viljava, A.O.I. Krause, J. Mol. Catal. A: Chem. 27 (2007) 107.
[21] B.M. Reddy, A. Khan, Catal. Rev. 47 (2005) 257.
[22] R.K. Kaila, A. Gutierrez, R. Slioor, M. Kemell, M. Leskelä, A.O.I. Krause, Appl. Catal. B 84 (2008) 223.
[23] R.K. Kaila, A. Gutierrez, S.T. Korhonen, A.O.I. Krause, Catal. Lett. 115 (2007) 70.
[24] J.A. Moulijn, M. Makkee, A. van Diepen, Chemical Process Technology, Wiley, Weinheim, England, 2001, pp. 18.
[25] O. Ozturk, S. Ma, J.B. Park, J.S. Ratliff, J. Zhou, D.R. Mullins, D.A. Chen, Surf. Sci. 601 (2007) 3099.
[26] D.C. Cronauer, T.R. Krause, J. Salinas, A. Wagner, J. Wagner, Prepr. Pap. -Am. Chem. Soc., Div. Fuel Chem. 51 (1) (2006) 297.
[27] K.T. Jacob, S. Priya, Y. Waseda, Bull. Mater. Sci. 21 (1998) 99.
[28] J.H. Bitter, K. Seshan, J.A. Lercher, J. Catal. 176 (1998) 93.
[29] F.G.A. van der Berg, J.H.E. Glezer, W.M.H. Sachtler, J. Catal. 93 (1985) 340.
[30] J.R. Aittamaa, K.I. Keskinen, Flowbat-User's Instruction Manual. Laboratory of Chemical Engineering, Helsinki University of Technology, Espoo, Finland, 2000 .
[31] H.-Y. Cai, J.M. Shaw, K.H. Chung, Fuel 80 (2001) 1065.
[32] M. Ferrari, B. Delmon, P. Grange, Micropor. Mesopor. Mater. 56 (2002) 279.
[33] A. Roine, HSC for Windows 5.11, Outokumpu Research Oy, 2003.
[34] H. Jiang, H. Yang, R. Hawkins, Z. Ring, Catal. Today 125 (2007) 282.
[35] S. Derrouiche, D. Bianchi, Langmuir 20 (2004) 4489.